

Effect of an induced mild form of hyperhomocysteinemia on the function and β -amyloid peptide accumulation in the rat heart: Is there some heart-brain axis?

Maria KOVALSKA ¹, Petra HNILICOVA ², Katarina LESKOVA MAJDOVA ³, Zuzana TATARKOVA ³, Dagmar KALENSKA ⁴, Jan LEHOTSKY ³

¹Department of Histology and Embryology, Jessenius Faculty of Medicine, Comenius University in Bratislava, 03601 Martin, Slovakia, ²Biomedical Center Martin, Jessenius Faculty of Medicine, Comenius University in Bratislava, 03601 Martin, Slovakia, ³Department of Medical Biochemistry, Jessenius Faculty of Medicine, Comenius University in Bratislava, 03601 Martin, Slovakia, ⁴Department of Anatomy, Jessenius Faculty of Medicine, Comenius University in Bratislava, 03601 Martin, Slovakia.

Correspondence to: Prof. RNDr. Jan Lehotsky, Department of Medical Biochemistry, Jessenius Faculty of Medicine, Comenius University, Mala Hora 4D, 036 01 Martin, Slovak Republic.
TEL: +421-43-2633-821, E-MAIL: jan.lehotsky@uniba.sk

Submitted: 2024-11-03 *Accepted:* 2024-12-21 *Published online:* 2025-03-31

Key words: **hyperhomocysteinemia; heart-brain axis; cardiomyocytes; A β -peptide; apoptosis**

Abstract

OBJECTIVES: Modifying risk factors remains a primary strategy for preventing cardio- and cerebrovascular disease (CVD), and although treatment options for modifiable factors have expanded, effective management in practice remains challenging. Studies link Alzheimer's disease (AD) with CVD manifested by hypertension and intra- and extra-cranial atherosclerosis and arteriosclerosis. Elevated plasma homocysteine (Hcy) level is recognized as a CVD risk factor, with even mild elevations linked to endothelial dysfunction. However, the exact role of Hcy in CVD is still uncertain. Moreover, AD-mediated degeneration of the brain's neuro-signalling pathways, together with a potential peripheral amyloid accumulation, may have detrimental effects on other organs, including the heart.

MATERIAL & METHODS: In this study, Wistar rats received daily subcutaneous Hcy injections (1.2 μ mol/g/day) for three weeks. After the treatment, the animals were sacrificed, and their hearts were perfused on a Langendorff system with Krebs – Henseleit solution. The hearts were fixed in formalin and prepared for histological and immunohistochemical analyses.

RESULTS: The hHcy group showed increased perfusion pressure, reduced left ventricular end-diastolic pressure (LVDP), and lower heart contraction and relaxation indexes (+LV dP/dt and -LV dP/dt). Structural changes in the Hcy-treated group included increased cell volume, cardiomyocyte disintegration, and elevated programmed cell death occurrence. Immunohistochemical results revealed β -amyloid peptide deposits in Hcy-treated animals.

CONCLUSION: These findings indicate that hHcy affects heart microcirculation and cardiomyocytes, leading to changes in heart structure and function. These changes could be linked to the progression of the brain's neuro-signaling pathways dysregulation and likely future neurodegeneration.

Abbreviations:

β -amyloid (A β), Alzheimer's disease (AD), cardiovascular diseases (CVD), homocysteine (Hcy), hyperhomocysteinemia (hHcy), left atrium (LA), left ventricle (LV), reactive oxygen species (ROS).

INTRODUCTION

Cardiovascular diseases (CVD) are the dominant cause of mortality worldwide, with an ever-increasing prevalence. From the point of view of etiology, these are multifactorial diseases caused by many risk factors, including lifestyle and the associated diet (Cai *et al.* 2024). Nowadays, inappropriate eating habits include foods rich in sulfurous amino acids, such as methionine. It is an essential amino acid, and with its high intake, patients can develop hyperhomocysteinemia (hHcy; González-Lamuño *et al.* 2024). Homocysteine (Hcy) is an intermediate product of the metabolic conversion of methionine to cysteine (Jakubowski 2019; Lehotsky *et al.* 2021). It is widely recognized in clinical practice as a risk factor for CVD development (Unadkat *et al.* 2024). Moreover, studies link most neurodegenerative diseases, such as Alzheimer's disease (AD), with CVD manifested by hypertension (Carnevale *et al.* 2016; Lennon *et al.* 2019) and intra- and extracranial atherosclerosis and arteriosclerosis. Both AD and CVD are progressive diseases with decades-long incubation periods before clinical manifestation (Saeed *et al.* 2023).

Many studies have confirmed the correlation between the increased concentration of hHcy in patients' plasma and ischemic heart disease, which most often arises based on the progression of the atherosclerotic vascular process (Zhu *et al.* 2023; Unadkat *et al.* 2024). It is a continuous inflammatory involvement of the tunica intima of blood vessels with an increase in plasma permeability, lipid plaque accumulation, and subsequent fibrotisation and calcification. Hcy potentiates the development of CVD by several pathomechanisms (Jakubowski 2019), while cardiomyocyte damage might be directly proportional to its serum concentration. Studies confirm that an increase in plasma Hcy concentration of 5 $\mu\text{mol/l}$ is associated with a 33.6 % increase in the risk of coronary heart disease and a 59 % increase in the risk of heart attack (Fan *et al.* 2017). Likewise, hHcy increases systolic and diastolic blood pressure and causes a decrease in vascular compliance manifested in hypertension (Chen *et al.* 2018), which could lead to neurodegeneration development (Saeed *et al.* 2023).

Furthermore, Hcy, as a stress factor, triggers the cellular apoptotic pathway. The most common occurrence of Hcy-induced apoptosis in endothelial cells and neurons is due to the accumulation of free oxygen radicals (ROS – reactive oxygen species; Jakubowski 2019; Lehotsky *et al.* 2021; Zhang *et al.* 2021). While there are currently only a limited number of studies that describe the effect of Hcy on cardiomyocytes, understanding the pathogenesis of damage to these cells could pave the way for more effective therapies for patients with CVD.

Moreover, the newly described cardiogenic dementia based on the heart-to-brain connection due to the compromised blood flow to the brain, amyloid, or atherosclerotic angiopathy may offer hope for improved treatment strategies for patients with ingoing AD (Liu *et al.* 2024).

Based on these findings, we monitored the effect of an increased plasma concentration of Hcy on myocardial tissue morphology and functional parameters using the Langendorff perfusion system. We also analyzed the presence of cellular apoptosis, its localization, and the abundance of apoptosis-specific protease (cleaved) caspase 3 in cardiomyocytes.

Our previous works on a similar hHcy-model with a lower daily dose of Hcy demonstrated AD-like pathology in the rat brain parenchyma and brain blood vessels amyloidosis (Kovalska *et al.* 2018, 2019). The AD-mediated degeneration of the brain's neuro-signaling pathways, together with a potential peripheral amyloid accumulation, may also result in the derangement of the peripheral nervous system, culminating in detrimental effects on other organs, including the heart (Elia *et al.* 2023). However, whether and how AD-like pathology modulates cardiac function, morphology, and amyloidosis remains unknown. Here, we report that cardiomyocyte apoptosis, β -amyloid peptide 42 (A β 42) accumulation, and histomorphological and functional changes occur in the heart of wild-type rats in hHcy conditions modeling AD-like pathology.

MATERIAL & METHODS*Experimental Procedures with Mild hHcy Induction*

This study adhered to the Animal Care and Health guidelines set by the State Veterinary and Food Department of Slovakia (approval number 3033-3/2020-220 for animal experiments). It was conducted by Directive 2010/63/EU of the European Parliament and Council concerning protecting animals used in scientific research. Given the antioxidant, anti-inflammatory, and cardioprotective properties of estrogen (Iorga *et al.* 2017; Aryan *et al.* 2020), adult male Wistar rats (sourced from Dobra Voda, Bratislava, Slovakia) were selected for the study. The rats were 4 to 6 months old, with weights ranging from 430 to 490 grams (average weight 460 g). Sixteen rats were included and kept in air-conditioned rooms under standard conditions, maintaining a temperature of 22 ± 2 °C with a 12-hour light/dark cycle. Food and water were freely available at all times. Eight of the sixteen rats were subjected to a mild hHcy for 21 days. To induce mild hHcy, D, L-Hcy (Sigma-Aldrich, Bratislava, Slovakia) was dissolved in a 0.85% (w/v) NaCl solution and adjusted to a pH of 7.4. The Hcy solution, at a dose of 0.6 μmol per gram of body weight, was administered subcutaneously in the dorsal region (in the loose skin over the flank) twice a day at 7 a.m. and 3 p.m. over 21 days as described by Matté *et al.* (2010). Following subcutaneous injection, Hcy

crosses the blood-brain barrier and reaches its peak concentration in the cerebrum and parietal cortex between 15 and 60 minutes (Streck *et al.* 2002; Matté *et al.* 2010). The dosage of Hcy was calculated based on pharmacokinetic parameters previously established by Martins *et al.* (2005), which achieved plasma Hcy levels in rats comparable to those in patients with mild hHcy (Streck *et al.* 2002). Meanwhile, the control group (C rats, n = 8) did not undergo the induction of mild hHcy. After assessing the daily Hcy injection intake, rats underwent mild hHcy induction, as described in our previous studies (Pavlikova *et al.* 2011; Petráš *et al.* 2017; Kovalska *et al.* 2018, 2019). The animals' weights were recorded on days 0, 7, 14, and 21 of the experiment. On the 22nd day, blood samples (1.0 – 1.5 ml) were obtained from the retroorbital venous plexus. After collecting the blood samples, they were promptly cooled on ice, centrifuged, and the resulting supernatant – plasma – was stored at -80 °C. We assessed the total plasma Hcy levels, following established protocols from our previous studies (Petráš *et al.* 2017; Kovalska *et al.* 2018, 2019) as well as other experimental (Sudduth *et al.* 2017; Weekman *et al.* 2019) and clinical works (Labinjoh *et al.* 2001; Nestel 2003) for evaluating the mild hHcy induced by the Hcy subcutaneous injections treatment.

On day 22, both experimental groups were decapitated, and their hearts were carefully dissected and prepared for future analysis. Hearts from 4 animals from both groups (C and hHcy) underwent histological and immunohistochemical analyses. Another four hearts from both groups (C and hHcy) were applied to the Langendorff perfusion system, and their functional parameters were examined.

Langendorff's perfusion system and preparation of isolated hearts

Each animal was humanely decapitated following 5 min of anesthesia of 3.5 % sevoflurane in an O₂/NO mixture (1:2), and then its heart was operated on. The heart was transferred in a physiological solution (0.15 mmol/l NaCl) with heparin, rapidly (within 1 minute) cannulated through the aorta to ensure the maintenance of spontaneous sinus rhythm and continuously perfused with Krebs-Henseleit solution (135 mmol/l NaCl; 5.4 mmol/l KCl; 0.9 mmol/l MgCl₂; 24 mmol/l NaHCO₃; 1.2 mmol/l NaH₂PO₄; 1.8 mmol/l CaCl₂; 10 mmol/l glucose; pH 7.4) saturated with 95 % O₂ and 5 % CO₂ at 37°C and constant pressure of 73 mmHg. Isovolumetric left ventricular pressure was recorded with a latex balloon connected to a pressure transducer. The balloon was inserted into the left ventricle through the left atrium, and its volume was adjusted to achieve an initial left ventricular end-diastolic pressure of 8-12 mmHg. In the experiment, we used a Langendorff perfusion system (AD Instruments, New Zealand) connected to a computer to record for 20 minutes and evaluate all hemodynamic parameters

using the LabChart Software (ADInstruments, Spechbach, Germany).

Histological and immunohistochemical staining of paraffin sections

The analyzed material was processed in the experiment according to standard tissue preparation protocols using the paraffin method (Carlson 2014), and it was subsequently stored in paraffin blocks. Ten 2 – 4 µm thick sections were cut from each paraffin block using a rotary microtome (Leica Biosystems, Germany) for evidence of histomorphological changes (hematoxylin-eosin – H&E), apoptosis (cleaved caspase 3) and the presence of amyloid deposits (anti-Aβ-peptide). Individual sections were subsequently transferred to the surface of an aqueous solution heated to 51°C. Heat treatment ensured the straightening of the section before placing it on a glass slide (TOMO® IHC Adhesive Glass Slide, Matsunami Glass Ind., Ltd., Japan). The slides with the sections were placed in a thermostat (Binder, Germany) at a temperature of 59 °C for 1 hour to avoid possible sliding of the tissue during immunohistochemical staining. First, it was necessary to deparaffinize the slides with applied sections. When the paraffin was removed, the slides underwent basic histological staining (H&E) according to the standard protocols (Carlson 2014) and immunohistochemical analyses. Immunohistochemical methods included revitalization of the antigen for 20 minutes in a citrate buffer with a high pH (EnVision FLEX Target Retrieval solution, Dako Agilent, CA, United States; for both antibodies) form, which was heated to 96 °C. After cooling the slides, we washed them in PBS solution. Sections were further incubated for 10 minutes in 3 % H₂O₂ solution (blocking non-specific binding) and washed with PBS solution. We then allowed the sections to be incubated for 60 minutes with the primary antibody (cleaved) caspase 3 at the dilution 1:500 (rabbit polyclonal, ab2320, Abcam, Cambridge, UK). An additional antibody used in this work was anti-Aβ1 – 42 peptide (rabbit polyclonal, XHU-50U G, Millipore, MA, United States) in a dilution of 1:35, which was used to detect the presence of amyloid deposits. The excess antibody was washed away using a PBS solution. In the next step, we applied 100 µl of the detection system (Goat Anti-Mouse Anti-Rabbit IgG/IgM H&L, AB2891; Abcam, Cambridge, UK) to each section, which we left to act until a brown reaction appeared. Sections were washed with distilled water, stained with hematoxylin (Dako Agilent, CA, United States) to highlight cell nuclei, cleared with xylene, and placed in a mounting medium (Entellan, Millipore, MA, United States).

Quantitative Image Analysis

Serial longitudinal sections of the heart, each 2 – 4 µm thick, were taken with every 10th section selected, covering approximately a 2 mm span. These sections were prepared and stained for analysis. For quanti-

tative imaging, two independent, blinded observers conducted cell counts in the longitudinal heart sections, selecting three random fields per section for a double-blind evaluation. Data from six sections per animal were combined and multiplied by 3 (representing three fields per left atrium region), resulting in the total positive cell count for the left atrium and ventricle.

Image brightness and contrast adjustments were standardized using Adobe Photoshop CS3 Extended, version 10.0 for Windows (Adobe Systems, CA, USA). Tiff-formatted longitudinal heart section images from both experimental groups (C and hHcy) were analyzed using ImageJ software (NIH, MD, USA). The RGB images were converted to 8-bit grayscale, and thresholds were set between 13 to 255 pixels. Particle analysis was applied with size settings from 0 mm² to infinity without shape constraints. The counting frame measured 0.6 × 0.6 mm, and cell counts were performed manually with an automated count comparison, yielding a 3 – 5% variation. Results were recorded as the total cell count per optical field (0.6 × 0.6 mm).

Statistical Analysis

Image analysis data and functional parameters underwent statistical analysis using SPSS software (Version 15.0; IL, USA), where the Kolmogorov–Smirnov test assessed data normality, with $p < 0.05$ as the significance threshold. GraphPad Prism software, version 6.01 for Windows (La Jolla, CA, USA), was utilized to analyze heart longitudinal section images. Group differences between control (C) and hHcy groups were examined using an unpaired t-test with Welch's correction, setting significance at $p < 0.05$.

RESULTS

Functional parameters

In the hHcy-induced group, we observed a statistically significant increase in perfusion pressure values to 86.16 ± 4.52 during the experiment compared to the physiological range of 73.14 ± 2.22 mmHg in the control group. This increase represented 17.8 % ($p < 0.05$). The pulse frequency in the hHcy group considerably increased compared to the control group, but this ascent was not statistically significant. It is necessary to mention that in all hHcy animals, it was hard to measure this value correctly due to sporadic arrhythmia. Evaluation of the

left ventricular contraction rate (+LV dp/dt) and relaxation (-LV dp/dt) indices in the hHcy group showed a reduction of +LV dp/dt by 30.9 % ($p < 0.05$) and of -LV dp/dt by 17.4 % ($p < 0.05$) compared to control. Surprisingly, the end-left ventricular pressure (LVDP) was 23.4 % ($p < 0.001$) lower in the hHcy group compared to the control (Table 1).

Histomorphological analyses

Based on the physiological parameter analysis results, we focused on the left part of the heart for routine histological and immunohistochemical analyses. We used each animal's left ventricle (LV) and left atrium (LA; Figure 1) for observation.

With standard histological H&E staining, no pathological changes were observed in the control group (C). Cardiomyocytes are polygonal cells with a cylindrical appearance with a centrally located nucleus. The perinuclear cytoplasm does not contain myofibrils but is rich in cell organelles. The dark-colored lines at the interface of cardiomyocytes represent discs (Figure 1 – arrowhead), which provide a connection from cell to cell into the so-called functional syncytium.

In the hHcy group affected by mild hHcy (21 days, $c = 1.2 \mu\text{mol/g}$ of the animal/day), we detected the presence of hypertrophic cardiomyocytes during H&E staining in microscopic specimens (Figure 1 – red arrow). We observed lightening and enlargement of perinuclear spaces of individual cardiomyocytes (Figure 1 – yellow empty arrow). As a result of cellular hypertrophy (Figure 1 – red arrow), the nuclei of cardiomyocytes were large, pale, and morphologically changed (Figure 1 – yellow arrow). We ascertained a slight disintegration of contractile proteins within individual cells (Figure 1 – green empty arrow). Additionally, we have detected several shrunk cardiomyocytes with a subsequent decrease in their diameter (Figure 1 – green arrow), likely due to the onset of ongoing apoptosis (Figure 1 – green arrow). Furthermore, we observed a much paler cytoplasm in the hypertrophic cardiomyocytes, likely due to the effect of oxidative stress of hHcy on the mitochondria and smooth endoplasmic reticulum.

Immunohistochemical analyses

Using the cleaved caspase 3, which explicitly identifies cells subjected to cell death, we demonstrated a statis-

Tab. 1. Hearts functional parameters of control and hHcy groups

Parameters Groups	Coronary flow (ml/min)	Perf. pressure (mmHg)	Pulse frequency/min	+LV dp/dT (mmHg/s)	-LV dp/dT (mmHg/s)	LVDP (mmHg)
C	17.86 ± 1.92	73.14 ± 2.22	205.12 ± 43.99	1721.68 ± 276.01	945.69 ± 215.01	95.14 ± 7.89
hHcy	16.64 ± 0.91	86.16 ± 4.52 *	260.31 ± 59.47	1190.34 ± 7.02 *	781.42 ± 91.09 *	72.88 ± 2.07 ***

Annotations: +LV dp/dT – left ventricular contraction rate; -LV dp/dt – left ventricular relaxation; LVDP – end-left ventricular pressure

tically significant and more intense positivity in LA with diffuse positivity at the peripheral myocardium in LV (Figure 2 – first column), and its localization was mainly in the nucleus. We detected an increase in cleaved caspase 3+ cardiomyocytes of LV (36.7-fold; $p < 0.001$) with a massive rise in LA (79.3-fold; $p < 0.001$; Figure 2).

The statistical significance between positivity in LV and LA reached a 2.16-fold increase ($p < 0.001$; Figure 2 – last column). Using immunohistochemical detection of the presence of A β -peptide, we also quantitatively evaluated the number of A β 42+ cardiomyocytes in the hHcy group. Compared to the control group, we observed a statistically significant, 38-fold ($p < 0.05$)

increase in A β 42+ cardiomyocytes with diffuse, more peripheral localization in the LV of the hHcy group. In the LA analysis, we recorded a 146-fold ($p < 0.001$) increase in the number of A β 42+ cardiomyocytes compared to the control. We also found striking, statistically significant differences between LA and LV in the hHcy group. The increase in the post of A β 42+ cardiomyocytes per field in the LA hHcy group increased 3.8-fold ($p < 0.001$) compared to LV (Figure 2). The localization of A β -peptide was in the perinuclear area (Figure 2 – brown arrow) of cardiomyocytes. Besides, we found A β 42+ in the endothelium, tunica intima of small blood vessels, and platelets (Figure 3 – brown empty arrow).

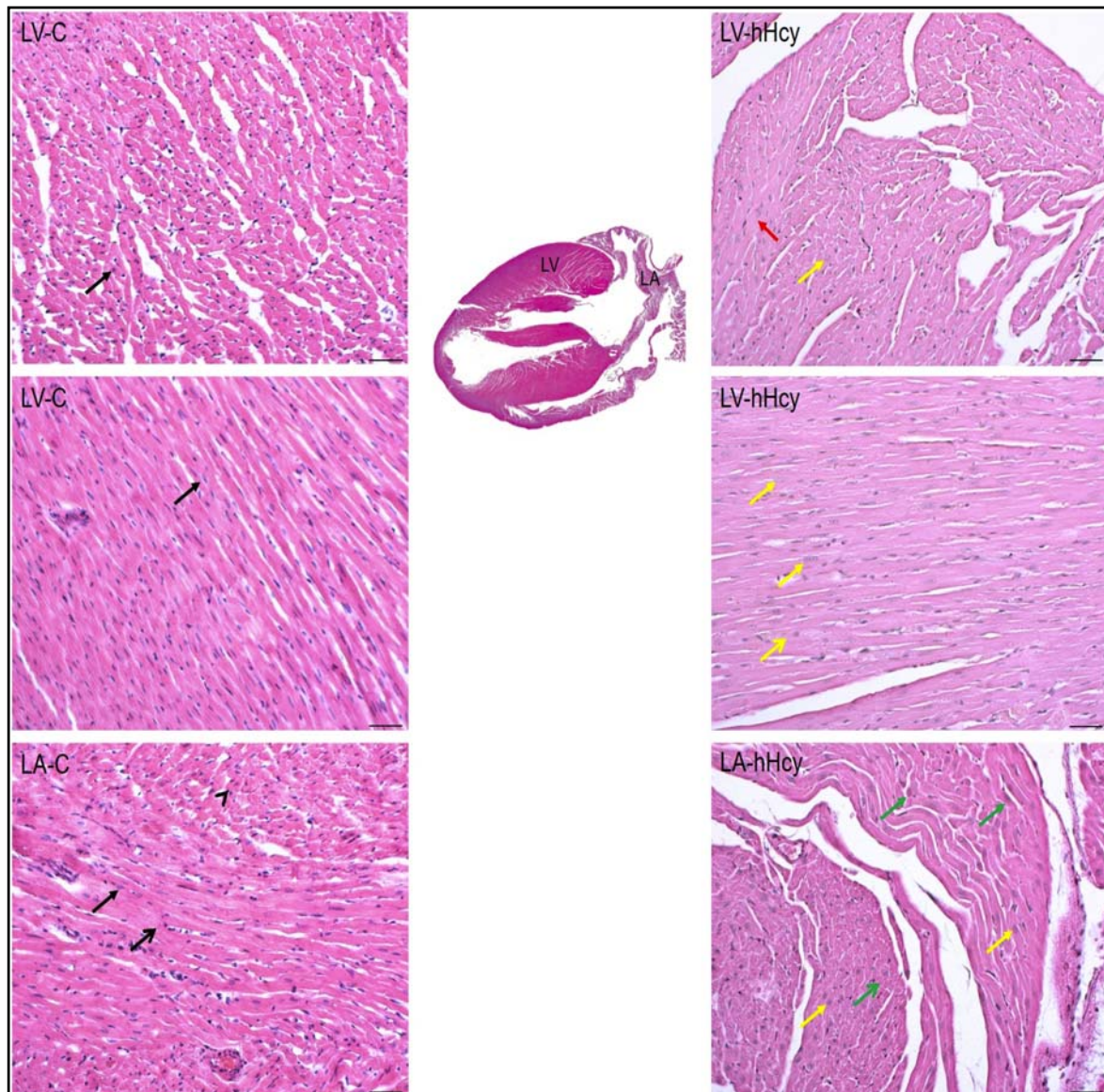


Fig. 1. Microphotographs of rat myocardium in the cross (first line) and longitudinal (second line) section stained with H&E (magnification: 200x) in control (C) and hHcy groups.

In the center of the figure is a representative photograph of a longitudinal section of a rat heart stained with H&E.

Annotations: Black arrow – normal nuclei; black empty arrow – intercalated disc; black arrowhead – normal cardiomyocyte; red arrow – hypertrophic cardiomyocyte; yellow arrow – hypertrophic nuclei; yellow empty arrow – swelling and lightening of perinuclear space; green empty arrow – the disintegration of contractile proteins; green arrows – shrinking cardiomyocytes; LV – left ventricle, LA – left atrium. Bar = 20 μ m.

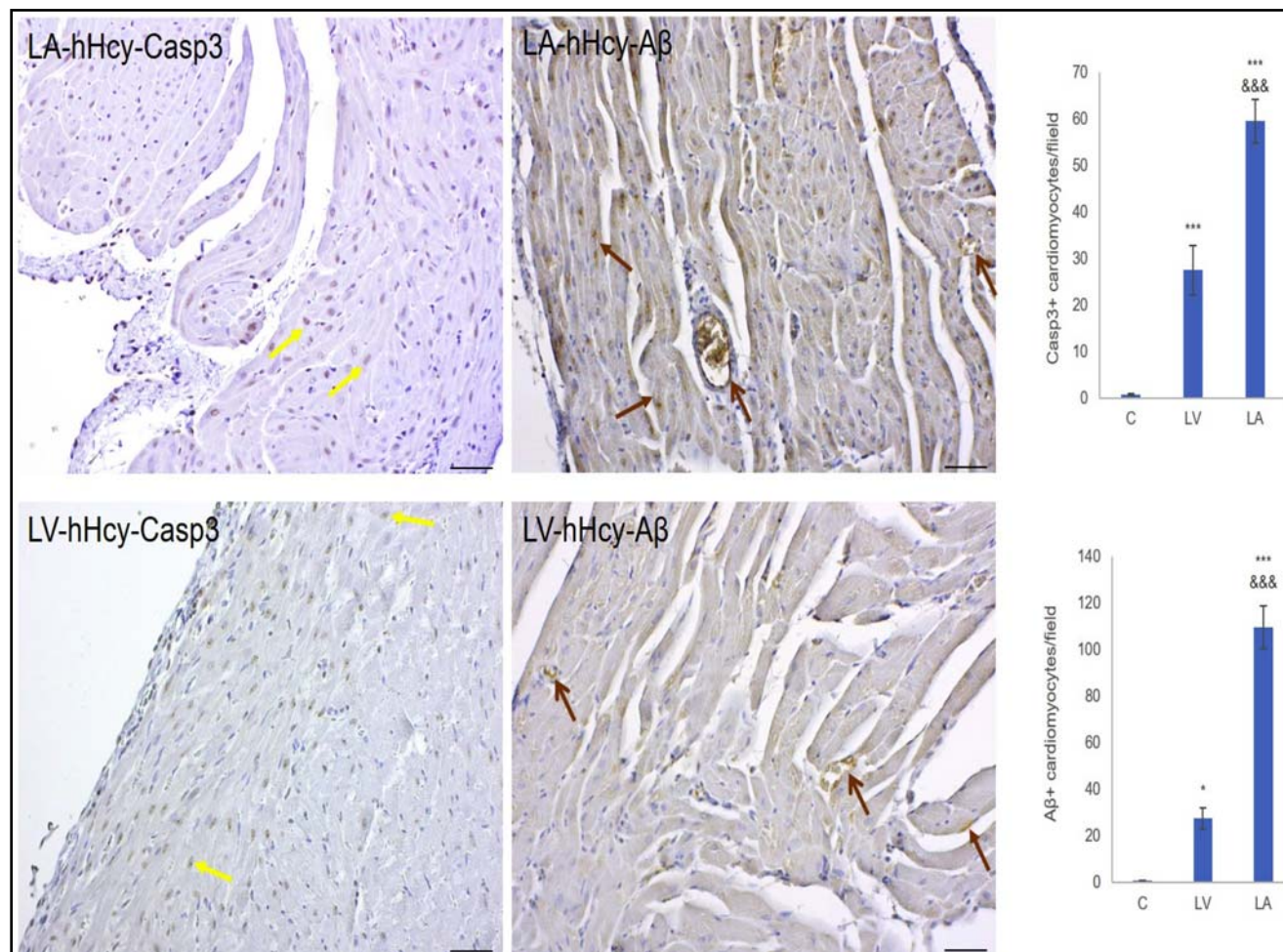


Fig. 2. Representative microphotographs of rat myocardium with immunohistochemical analyses of the presence of apoptosis and A β -peptide in the myocardium of the hHcy group with statistical evaluation
 Demonstrative microphotographs of Casp3+ and A β 42+ cardiomyocytes of rat heart myocardium in the LA and LV sections or rat myocardium (first two columns). Bar = 20 μ m; n = 4/group. The number of cleaved Casp3+ and A β + cardiomyocytes in the LV and LA of the rat heart myocardium in the control and hHcy group (last column). The significance of group mean differences was evaluated by unpaired t-test. Results are presented as mean \pm SD, n=4/group, * p < 0.05, and *** p < 0.001 versus the control group; &&& p < 0.001 versus LA
Annotations: + – positivity; Yellow arrows – positive nuclei; brown arrows – A β 42+; brown empty arrows – A β 42 presence in blood vessels (lumen, endothelium and tunica intima); Casp3 – caspase 3; LV – left ventricle, LA – left atrium

DISCUSSION

Over the past two decades, research has identified Hcy as an independent risk factor for CVD, thrombosis, vasculopathies, systemic diseases, and cognitive disorders. However, its mechanisms are still not fully understood (Yin *et al.* 2022; Unadkat *et al.* 2024). Hcy's association with CVD may involve endothelial and vascular smooth muscle dysfunction, platelet defects, and coagulation changes (Kolling *et al.* 2011). Hcy-induced oxidative stress and reduced nitric oxide (NO) availability are linked to atherosclerosis and thrombosis (Jakubowski, 2019), while Hcy also disrupts vasodilator synthesis and promotes vascular wall remodeling, impacting elasticity and diastolic function (Ganguly & Alam 2015). Recent studies suggest Hcy may impair cardiac muscle and remodeling, as seen in renal disease patients and animal models (Zhang *et al.* 2021; Zhu *et al.* 2023). Additionally, Hcy affects NO-dependent cardiac oxygen regula-

tion (Wang *et al.* 2012) and is associated with dementia and AD through its ties to atherosclerosis (Lennon *et al.* 2019; Saeed *et al.* 2023; Liu *et al.* 2024).

Our results show that induced hHcy leads to significant declines in cardiac function, marked by both systolic and diastolic dysfunction. Few studies have examined heart function parameters during hHcy. Timkova *et al.* (2016) similarly found myocardial contractile dysfunction in rats after two weeks of Hcy exposure. Wang *et al.* (2012) also observed that Hcy impaired cardiomyocyte contractility in vitro without affecting Ca²⁺ transients, possibly due to decreased sensitivity of myofilaments to Ca²⁺. Myofilament protein phosphorylation may regulate this interaction, as Liao *et al.* (2002) and Vahebi *et al.* (2007) found that dephosphorylation of α -tropomyosin via mitogen-activated protein kinase (MAPK/p38) reduces sarcomere tension and ATPase activity, potentially contributing to Hcy-induced contractile dysfunction, which supports our findings.

In this study, examination of the Hcy's direct effects on the myocardial structure has demonstrated specific changes such as hypertrophy of cardiomyocytes, perinuclear space, and cytoplasm lightening with mild disintegration of contractile proteins and shrinking of individual cardiomyocytes. These align with the results of Joseph *et al.* (2003), who found that moderate hHcy in Wistar rats over 10 weeks led to myocardial remodeling, including cardiomyocyte hypertrophy and interstitial collagen build-up – more likely a compensatory response to early cell loss. Joseph *et al.* (2003) also showed that hHcy alone could induce pathological hypertrophy, ventricular remodeling, and diastolic dysfunction. This aligns with other studies linking hHcy to oxidative stress and mitochondrial damage (Petráš *et al.* 2017; Jakubowski 2019; Yin *et al.* 2022), potentially explaining reduced cytoplasmic staining in our results, as similar mechanisms involving endoplasmic and mitochondrial stress contribute to myocardial apoptosis (Zhang *et al.* 2021).

Apoptosis is critical in both CVD and AD pathology (Saeed *et al.* 2023) and may drive cardiac dysfunction and heart failure (Zhang *et al.* 2021; Ying *et al.* 2022; Cai *et al.* 2024). In this study, we found apoptosis in the LV, worsening LA outcomes under hHcy conditions, consistent with prior studies on functional deterioration (Wang *et al.* 2012; Timkova *et al.* 2016; Yin *et al.* 2022). Schurgers *et al.* (2016) showed that CVD patients have significantly higher apoptosis levels, making it a potential biomarker for mortality prediction in heart failure with possible links to the subsequent brain neurodegeneration. Cardiomyocyte loss further predicts cardiac dysfunction (Zhu *et al.* 2023; Cai *et al.* 2024). Understanding apoptosis in hHcy-related cardiomyopathy may inform interventional strategies, though more evidence is needed to clarify these pathways for clinical application.

A β 42, the primary component of pathological cerebrovascular amyloid deposits, was used in this study. Using immunohistochemistry, we detected incoming amyloidogenesis in the myocardium of wild-type rats, observing A β 42+ cardiomyocytes in the LV and LA. A β 42+ was visualized in the vascular endothelium, vessel walls, and within cardiomyocytes. Given the presence of A β -peptides in platelets and peripheral circulation, we also localized A β 42 in the vessel lumen (Figure 2 – brown empty arrows; Jang *et al.* 2022). Troncone *et al.* (2016) similarly confirmed by echocardiographic measurements of myocardial function that patients with AD present with an anticipated diastolic dysfunction and intramyocardial deposits of A β 42 in LV of AD patients. Zhu *et al.* (2023) determined the associations of plasma A β 40 and A β 42 with echocardiographic measurements of cardiac dysfunction and with incident heart failure in the general population. They proved that higher levels of A β 40 were associated with worse cardiac function and a higher risk of new-onset heart failure in the general population, in partic-

ular among men. The stronger association observed with A β 40 may stem from A β 42's tendency to escape from the bloodstream and accumulate in vascular beds and tissues (Lewis *et al.* 2006). Additionally, the accumulation of A β 42 in cardiac mitochondria and its associated reduction in complex I respiration in cardiomyocytes mirrors certain aspects of A β 42 seen in AD (Hall *et al.* 2024), supporting our outcomes. Moreover, elevated systemic A β 42 altered cardiac glucose metabolism, leading to reduced glucose clearance. Cardiac glucose metabolism impairment affects heart function (Dai *et al.* 2020; Cluntun *et al.* 2021). Reflecting on these observations, Hall *et al.* (2024) demonstrated that administering A β 42 to healthy mice resulted in significant defects in diastolic and systolic functions, corresponding to our study's results. The deposition of amyloid fibers from circulating A β -peptides in the heart may lead to subsequent cardiac dysfunction in AD patients (Troncone *et al.* 2016). This may occur through basolateral-to-apical transport of soluble A β -peptides or blood-brain barrier disruption, allowing A β -peptides leakage into circulation, as observed in human and AD mouse models (Pitschke *et al.* 1998; Ujiie *et al.* 2003). Significant levels of A β -peptides in peripheral blood and platelets have also been linked to worsened coronary artery disease, suggesting that A β -peptides accumulation in the heart may impair myocardial function in AD, indicating a more profound brain-to-heart pathological link beyond its vascular effects (Troncone *et al.* 2016). This mechanism aligns with findings of A β -peptides toxicity in cardiomyocytes (Gianni *et al.* 2010; Troncone *et al.* 2016) and neurons (Kovalska *et al.* 2018, 2019). Amyloid proteins like A β -peptides activate proinflammatory and necrotic responses (Parry *et al.* 2015), potentially further impacting myocardial function in hHcy conditions. Our results support the new hypothesis of cardiogenic dementia and align with Jang *et al.* (2022), who demonstrated that A β -toxicity is potentiated by Hcy and its adverse oxidative and excitotoxic effects. An increase in Hcy concentration potentiates an increase in its levels.

Our results support the suggestion that the Hcy-induced dysregulation of the brain's neuro-signaling pathways also influences the heart in the “heart-brain axis” and has a potential implication for both the cardiac and especially AD pathologies. The development of therapies that modify disease progression is challenging, partly because AD has a long preclinical phase. This phase begins in midlife, presenting a significant opportunity to identify and optimize risk factors for AD (Saeed *et al.* 2023).

CONCLUSION

Our results bring a novel understanding of the heart-brain connection, revealing that these organs interact through neurovascular and humoral pathways, forming a heart-brain axis (Lennon *et al.* 2019), which can be

affected by Hcy. Our study documented that mild hHcy in wild-type rats led to functional cardiac changes, hypertrophy of cardiomyocytes, activation of apoptosis, and accumulation of A β 42, one of the critical components in AD-like pathology. This highlights the need for interdisciplinary collaboration to develop better diagnostic tools and identify high-risk groups, potentially informing treatments for AD-related dementias and CVD (Saeed *et al.* 2023; Liu *et al.* 2024). Our findings suggest therapeutic approaches that target diet and inhibit cardiomyocyte apoptosis may benefit CVD and early AD stages.

ACKNOWLEDGMENT

This study was supported by Grants VEGA 1/0035/25 and VEGA 1/0274/23. The authors thank Mrs. Greta Kondekova and Mrs. Agata Resetarova for their excellent help with histological and immunohistochemical procedures.

REFERENCES

- Aryan L, Younessi D, Zargari M, Banerjee S, Agopian J, Rahman S *et al.* (2020). The Role of Estrogen Receptors in Cardiovascular Disease. *Int J Mol Sci.* **21**(12): 4314.
- Cai K, Jiang H, Zou Y, Song C, Cao K, Chen S, *et al.* (2024). Programmed death of cardiomyocytes in cardiovascular disease and new therapeutic approaches. *Pharmacol Res.* **206**: 107281.
- Carlson FL (2014). *Histotechnology - A self-instructional text.* 3rd ed. Hongkong: ASCP press.
- Carnevale D, Perrotta M, Lembo G, Trimarco B (2016). Pathophysiological links among hypertension and Alzheimer's disease. *High Blood Press Cardiovasc Prev.* **23**: 3–7.
- Chen L, Wang B, Wang J, Ban Q, Wu H, Song Y, *et al.* (2018). Association between serum total homocysteine and arterial stiffness in adults: a community-based study. *J Clin Hypertens (Greenwich).* **20**(4): 686–693.
- Cluntun AA, Badolia R, Lettlova S, Parnell KM, Shankar TS, Diakos NA, *et al.* (2021). The pyruvate-lactate axis modulates cardiac hypertrophy and heart failure. *Cell Metab.* **33**(3): 629–648.e10.
- Dai C, Li Q, May HI, Li C, Zhang G, Sharma G, *et al.* (2020). Lactate Dehydrogenase A Governs Cardiac Hypertrophic Growth in Response to Hemodynamic Stress. *Cell Rep.* **32**: 108087.
- Elia A, Parodi-Rullán R, Vazquez-Torres R, Carey A, Javadov S, Fossati S (2023). Amyloid β induces cardiac dysfunction and neurosignaling impairment in the heart of an Alzheimer's disease model. *bioRxiv [Preprint]*. **11**: 2023.07.11.548558.
- Fan R, Zhang A, Zhong F (2017). Association between homocysteine levels and all-cause mortality: A dose-response meta-analysis of prospective Studies. *Sci Rep.* **7**: 4769.
- Ganguly P, Alam SF (2015). Role of homocysteine in the development of cardiovascular disease. *Nutr J.* **14**: 6.
- Gianni D, Li A, Tesco G, McKay KM, Moore J, Raygor K, *et al.* (2010). Protein aggregates and novel presenilin gene variants in idiopathic dilated cardiomyopathy. *Circulation.* **121**: 1216–26.
- González-Lamuño D, Arrieta-Blanco FJ, Fuentes ED, Forga-Visa MT, Morales-Conejo M, Peña-Quintana L, *et al.* (2024). Hyperhomocysteinemia in Adult Patients: A Treatable Metabolic Condition. *Nutrients.* **16**: 135.
- Hall LG, Czegez JK, Connor T, Botella J, De Jong KA, Renton MC, *et al.* (2024). Amyloid beta 42 alters cardiac metabolism and impairs cardiac function in male mice with obesity. *Nat Commun.* **15**(1): 258.
- Iorga A, Cunningham CM, Moazeni S, Ruffenach G, Umar S, Eghbali M (2017). The protective role of estrogen and estrogen receptors in cardiovascular disease and the controversial use of estrogen therapy. *Biol Sex Differ.* **8**(1): 33.
- Jakubowski H (2019). Homocysteine Modification in Protein Structure/Function and Human Disease. *Physiol Rev.* **99**(1): 555–604.
- Jang S, Chapa-Dubocq XR, Parodi-Rullán RM, Fossati S, Javadov S (2022). Beta-Amyloid Instigates Dysfunction of Mitochondria in Cardiac Cells. *Cells.* **11**(3): 373.
- Joseph J, Joseph L, Shekhawat NS, Devi S, Wang J, Melchert RB, *et al.* (2003). Hyperhomocysteinemia leads to pathological ventricular hypertrophy in normotensive rats. *Am J Physiol Heart Circ Physiol.* **285**(2): H679–86.
- Kolling J, Scherer EB, da Cunha AA, da Cunha MJ, Wyse AT (2011). Homocysteine induces oxidative-nitrosative stress in heart of rats: prevention by folic acid. *Cardiovasc Toxicol.* **11**(1): 67–73.
- Kovalska M, Tothova B, Kovalska L, Tatarkova Z, Kalenska D, Tomascova A, *et al.* (2018). Association of Induced Hyperhomocysteinemia with Alzheimer's Disease-Like Neurodegeneration in Rat Cortical Neurons After Global Ischemia-Reperfusion Injury. *Neurochem Res.* **43**(9): 1766–1778.
- Kovalska M, Tothova B, Kalenska D, Tomascova A, Kovalska L, Adamkov M, *et al.* (2019). Association of induced hyperhomocysteinemia with neurodegeneration in rat entorhinal cortex-hippocampal system after global brain ischemia: A progression of Alzheimer's disease-like pathological features. *Act. Nerv Super Rediviva.* **61**: 31–38.
- Labinjoh C, Newby DE, Wilkinson IB, Megson IL, Maccallum H, Melville V, *et al.* (2001). Boon, N.A.; Webb, D.J. Effects of acute methionine loading and vitamin C on endogenous fibrinolysis, endothelium-dependent vasomotion and platelet aggregation. *Clin Sci.* **100**: 127–135.
- Lehotsky J, Kovalska M, Baranovicova E, Hnilicova P, Kalenska D, Kaplan P (2021). Ischemic Brain Injury in Hyperhomocysteinemia. In: Pluta R, editor. *Cerebral Ischemia.* 1st ed. Brisbane: Exon Publications, p. 61–72.
- Lennon MJ, Makkak SR, Crawford JD, Sachdev PS (2019). Midlife hypertension and Alzheimer's disease: a systematic review and meta-analysis. *J Alzheimers Dis.* **71**: 307–316.
- Lewis H, Behr D, Cookson N, Oakley A, Piggott M, Morris CM, *et al.* (2006). Quantification of Alzheimer pathology in ageing and dementia: age-related accumulation of amyloid-beta(42) peptide in vascular dementia. *Neuropathol Appl Neurobiol.* **32**(2): 103–18.
- Liao P, Wang SQ, Wang S, Zheng M, Zheng M, Zhang SJ, *et al.* (2002). p38 Mitogen-activated protein kinase mediates a negative inotropic effect in cardiac myocytes. *Circ Res.* **90**(2): 190–6.
- Liu J, Xiao G, Liang Y, He S, Lyu M, Zhu Y (2024). Heart-brain interaction in cardiogenic dementia: pathophysiology and therapeutic potential. *Front Cardiovasc Med.* **11**: 1304864.
- Martins PJ, Galdieri LC, Souza FG, Andersen ML, Benedito-Silva AA, Tufik S, *et al.* (2005). Physiological variation in plasma total homocysteine concentrations in rats. *Life Sci.* **76**(22): 2621–2629.
- Matté C, Mussulini BH, dos Santos TM, Soares FM, Simão F, Matté A, *et al.* (2010). Hyperhomocysteinemia reduces glutamate uptake in parietal cortex of rats. *Int J Dev Neurosci.* **28**(2): 183–7.
- Nestel P (2003). Arterial stiffness is rapidly induced by raising the plasma homocysteine concentration with methionine. *Atherosclerosis.* **171**: 83–86.
- Parry TL, Melehani JH, Ranek MJ, Willis MS (2015). Functional amyloid signaling via the inflammasome, necrosome, and signalosome: new therapeutic targets in heart failure. *Front Cardiovasc Med.* **2**: 25.
- Pavlikova M, Kovalska M, Tatarkova Z, Sivonova-Kmetova M, Kaplan P, Lehotsky J (2011). Response of secretory pathways Ca²⁺ ATPase gene expression to hyperhomocysteinemia and/or ischemic preconditioning in rat cerebral cortex and hippocampus. *Gen Physiol Biophys.* **30**: 61–69.
- Petráš M, Drgová A, Kovalská M, Tatarková Z, Tóthová B, Křižanová O, *et al.* (2017). Effect of Hyperhomocysteinemia on Redox Balance and Redox Defence Enzymes in Ischemia-Reperfusion Injury and/or After Ischemic Preconditioning in Rats. *Cell Mol Neurobiol.* **37**: 1417–1431.

- 33 Pitschke M, Prior R, Haupt M, Riesner D (1998). Detection of single amyloid beta-protein aggregates in the cerebrospinal fluid of Alzheimer's patients by fluorescence correlation spectroscopy. *Nat Med.* **4**(7): 832–4.
- 34 Saeed A, Lopez O, Cohen A, Reis SE (2023). Cardiovascular Disease and Alzheimer's Disease: The Heart-Brain Axis. *J Am Heart Assoc.* **12**(21): e030780.
- 35 Schurgers LJ, Burgmaier M, Ueland T, Schutters K, Aakhus S, Hofstra L, et al. (2016). Circulating annexin A5 predicts mortality in patients with heart failure. *J Intern Med.* **279**(1): 89–97.
- 36 Streck EL, Matte C, Vieira PS, Rombaldi F, Wannmacher CMD, Wajner M, et al. (2002). Reduction of Na⁺,K⁺-ATPase activity in hippocampus of rats subjected to chemically-induced hyperhomocysteinemia. *Neurochem Res.* **27**(12): 1593–1598.
- 37 Sudduth TL, Weekman EM, Price BR, Gooch JL, Woolums A, Norris CM, et al. (2017). Time-course of glial changes in the hyperhomocysteinemia model of vascular cognitive impairment and dementia (VCID). *Neuroscience.* **341**: 42–51.
- 38 Timkova V, Tatarkova Z, Lehotsky J, Racay P, Dobrota D, Kaplan P (2016). Effects of mild hyperhomocysteinemia on electron transport chain complexes, oxidative stress, and protein expression in rat cardiac mitochondria. *Mol Cell Biochem.* **411**(1–2): 261–70.
- 39 Troncone L, Luciani M, Coggins M, Wilker EH, Ho CY, Codispoti KE, et al. (2016). A β Amyloid Pathology Affects the Hearts of Patients With Alzheimer's Disease: Mind the Heart. *J Am Coll Cardiol.* **68**(22): 2395–2407.
- 40 Ujiiie M, Dickstein DL, Carlow DA, Jefferies WA (2003). Blood-brain barrier permeability precedes senile plaque formation in an Alzheimer disease model. *Microcirculation.* **10**(6): 463–70.
- 41 Unadkat SV, Padhi BK, Bhongir AV, Gandhi AP, Shamim MA, Dahiya N, et al. (2024). Association between homocysteine and coronary artery disease-trend over time and across the regions: a systematic review and meta-analysis. *Egypt Heart J.* **76**(1): 29.
- 42 Vahebi S, Ota A, Li M, Warren CM, de Tombe PP, Wang Y, et al. (2007). p38-MAPK induced dephosphorylation of alpha-tropomyosin is associated with depression of myocardial sarcomeric tension and ATPase activity. *Circ Res.* **100**(3): 408–15.
- 43 Wang X, Cui L, Joseph J, Jiang B, Pimental D, Handy DE, et al. (2012). Homocysteine induces cardiomyocyte dysfunction and apoptosis through p38 MAPK-mediated increase in oxidant stress. *J Mol Cell Cardiol.* **52**(3): 753–60.
- 44 Weekman EM, Sudduth TL, Price BR, Woolums AE, Hawthorne D, Seaks CE, et al. (2019). Time course of neuropathological events in hyperhomocysteinemic amyloid depositing mice reveals early neuroinflammatory changes that precede amyloid changes and cerebrovascular events. *J Neuroinflamm.* **16**: 284.
- 45 Yin R, Wang H, Li C, Wang L, Lai S, Yang X, et al. (2022). Induction of apoptosis and autosis in cardiomyocytes by the combination of homocysteine and copper via NOX-mediated p62 expression. *Cell Death Discov.* **8**(1): 75.
- 46 Zhang N, Zhu L, Wu X, Yan R, Yang S, Jiang X, et al. (2021). The regulation of Ero1-alpha in homocysteine-induced macrophage apoptosis and vulnerable plaque formation in atherosclerosis. *Atherosclerosis.* **334**: 39–47.
- 47 Zhu F, Wolters FJ, Yaqub A, Leening MJG, Ghanbari M, Boersma E, et al. (2023). Plasma Amyloid- β in Relation to Cardiac Function and Risk of Heart Failure in General Population. *JACC Heart Fail.* **11**(1): 93–102.